Normalized Deep Learning Model for Classifying White Blood Cell

Ali Rakan Hasan Al-Jader [1], Neam Salim M. Sheet [2,*], Mazin N. Farhan [3], and Raid Rafi Omar Al-Nima [4]

[1] Department of Medical Device Technology Engineering, Mosul Technical Engineering College, Northern Technical University (NTU), Iraq
[2] Department of Network Technologies and Computer Software, Polytechnic College of Mosul, Northern Technical University, Iraq
[3] College of Health and Medical Techniques—Al-Dour, Northern Technical University, Iraq
[4] Department of Cybersecurity Technology Engineering, Technical Engineering College for Computer and AI, Northern Technical University, Iraq
Email: ali.rakan@ntu.edu.iq (A.R.H.A.); mti.lec40.neam@ntu.edu.iq (N.S.M.S.); Mazin.nadheer@ntu.edu.iq (M.N.F.); raidrafi3@ntu.edu.iq (R.R.O.A.-N.)
*Corresponding author

***Abstract*—Microscopic molecules, such as White Blood Cells (WBCs) or leukocytes, are used in somatic immunity. The classification of white blood cells into neutrophils, basophils, eosinophils, lymphocytes, and monocytes has become very important. With the development of artificial intelligence, which has become a powerful tool for enhancing efficiency and accuracy in the medical system, it has improved the quality of healthcare by supporting physicians in making immediate clinical decisions based on comprehensive evidence and knowledge. In this paper, a Normalized Deep Learning Model (NDLM) has been proposed to classify white blood cell types which can be considered as a developed Convolutional Neural Network (CNN), and it is a type of deep learning. It has a specific structure because the goal of our model is to classify white blood cells, and the cells are very precise. Therefore, we need small filters to capture the fine details of the cells. While medical images require fine filters, unlike nature images. The leukocyte types were classified with the result of a high accuracy of 96.19% by the suggested model in this paper for five types of white blood cells: neutrophils, basophils, eosinophils, lymphocytes, and monocytes. The second step of this paper is the comparison between the results of this paper and other papers, where the suggested model attained superior performance.**

***Keywords*—Convolutional Neural Network (CNN), deep learning, White Blood Cells (WBCs), classifier**

I. Introduction

The ability of Artificial Intelligence (AI) to learn from data sets and identify patterns imperceptible to the human eye enhances the accuracy and speed of timely diagnosis of blood cell abnormalities, which is a matter of life and death. This is very important in hematology.

Many advanced deep learning models can classify White Blood Cells (WBCs), in addition to many diseases, and detect them effectively without the need for medical specialists [1].

To classify WBCs into different types, we used Convolution Neural Network (CNN) to accurately identify the type based on nucleus shape and cell size, features that are difficult for humans to distinguish with high accuracy.

WBCs, also known as leukocytes, are made up of cytoplasm and nucleus, which are used to diagnose the patient's required information by counting leukocytes to detect several diseases like leukemia, cancer, and infections. WBCs have a good response to the immune system of the body and have different types including neutrophils, basophils, eosinophils, lymphocytes, and monocytes which are illustrated in Fig. 1 [2, 3].

The problem of automatic cell recognition still exists in a widely distributed medical landscape, and it is difficult to solve in traditional detection algorithms with low recognition rates and traditional networks with weaker feature extraction capabilities [4].

WBCs are an important part of the innate immune system. They have differences in texture, color, size and morphology, so we can solve the problem of classifying them using many development, models like combining Recurrent Neural Network (RNN) and CNN.

A CNN is a type of neural network that contains cells that extract features from inputs by moving them over with a small window called the kernel. The kernel moves in the entire input image, and the portion of the image captured with the kernel window is scanned for features identical to those learned by the cell. When it is applied sequentially, CNNs can extract both high-level and low-level features [5].

Leukemia is a type of blood and bone marrow cancer that develops when cells change shape. It can lead to anemia, an increased risk of infections, weakened immunity, and internal bleeding. So, immediate diagnosis

Manuscript received August 1, 2025; revised August 22, 2025; accepted October 27, 2025; published March 26, 2026.

is always a key component to successful therapy, while human calculations have possibilities of errors [6].

A quick, accurate, and more accessible technique for early diagnostics of leukemia cases is proposed by semantic segmentation of white blood cells based on UNet++, a DensNet-based technique, and a Marker-based Watershed (MW) algorithm to address the issues of WBC clustering and overlapping with the integration of Orderly Differential Equation (ODE) to extract image features using an encoder concept [7]. Medical image processing techniques and deep learning algorithms excel in the morphological characterization of WBCs and Red Blood Cells (RBCs) [7].

The researcher may choose one or more AI techniques for detecting diseases, such as segmentation techniques, classification methodologies, selection of descriptive characteristics, assessment criteria, and other methods [8].

AI applications have gone beyond detecting many diseases, tumors, and any defects that may occur in tissues, such as detecting glioma recurrence and the sensitivity and specificity of accurate prediction through machine learning mechanisms, especially the Support Vector Machine (SVM) model, which can have trouble telling the difference between alterations brought on by treatment and actual tumor recurrence. However, the promising performance of machine learning models and the powerful potential of clinical application achieve rapid diagnosis that ensures improved survival outcomes through improved diagnostic accuracy and decision making [9].

AI techniques have grown to be useful in neurosurgical decision-making, especially in situations with complicated or conflicting treatment options. Accurate prediction of the outcomes of endovascular therapy, microsurgery or conservative treatment of brain aneurysms can help in selecting and advising the patient and avoiding complications [10].

In patients with hydrocephalus, the Deep Learning (DL) models show proof-positive results in ventricular subdivision. Diagnoses mainly depend on 2-dimensional measurements and ratios, while traditional manual and semiautomatic ventricular segmentation is time-exhausting, and has poor flexibility in dealing with several radiological varieties [11].

II. Background

The optical microscope instrument is a high-precision instrument that counts WBCs, RBCs, Hemoglobin (HB), and platelet, which is called the complete blood count. It is used to improve the biomedical image of hematology analysis [12, 13].

Deep learning plays a major role in several fields such as disease diagnoses, speech recognition, biomedical imaging, etc. It considers the subtype of machine learning that is used to learn the high-level of pyramidal structure data [14].

In this paper, the CNN, the most popular deep learning model that uses mathematical matrices, is developed to detect the classification of leukocyte types. White blood cells are classified into five types: neutrophils, basophils, eosinophils, lymphocytes, and monocytes. The outcomes are contrasted with those of earlier research, including cutting-edge discoveries.

The blood picture, as shown in Fig. 1, has white blood cells, red blood cells, and platelets. The data set of blood images has been obtained in the color space RGB acquired from the analyzer CellaVision, DM96. The data of blood pictures contains 17,092 images with a size of 360×363 pixels and formatted in JPG. The data of WBCs types, neutrophils, basophils, eosinophils, lymphocytes, and monocytes were acquired from the blood picture to classify the WBCs types [15].

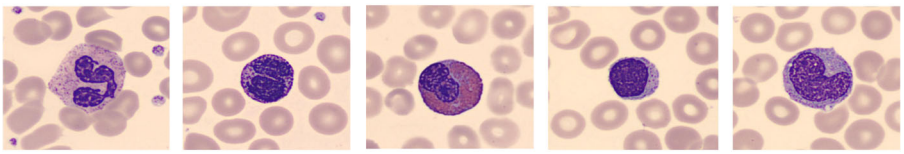

Fig. 1. Microscopic images of WBCs.

One popular DL network for image categorization is the Convolution Neural Network (CNN). Its principle depends on the principle of ANN. As the ANN grows, the number of invisible layers increases, leading to a complication process, thus, optimal outputs are obtained as a result. Layers of cells in the CNN are deeply supervised [16].

As mentioned, the Normalized Deep Learning Model (NDLM) is suggested here. Sequential NDLM layers consist of batch normalization layers before each of the convolutional, Rectified Linear Unit (ReLU), pooling, softmax, fully connected layers, softmax layers and then a classification layer [17].

Any layer in our model (NDEL) can be outlined as follows:

A. Batch Normalization Layer

This layer is autonomously natural for every single data channel on all values. My observations of the input image are normalized in this layer by calculating contrast σ^2 and the median on the space and the observation dimensions. Then the Eq. (1) will be as follows:

$$Z_{x,y} = \frac{I_{x,y} - median}{\sqrt{\sigma^2 + \epsilon}} \quad (1)$$

where: $Z_{x,y}$ is the output of the batch normalization layer of the input image I; x is the figure of rows; y is the figure of columns and ϵ is a constant. It improves mathematical

stability in case that σ^2 is very small. Consenting to the opportunity of median and σ^2 that are not suitable for batch normalizing processes.

The procedure modifies and uses Eq. (2) to assess the activation function values as a median = zero.

$$Z_{x,y} = \beta + \gamma Z_{x,y} \tag{2}$$

where: β refers to offset shifting and γ represents a scale factor. Both of these parameters are learnable, in which their values are updated throughout the training processes [18].

B. Convolutional Layer

Feature maps are produced by this layer after being extracted from every channel c_{in} in the preceding layer (c_{in} in the case of a greyscale WBC image equals 1). The feature map with a kernel (certain weight values) represents a convolved c_{in}. Typically, $k_w \times k_h \times c_{in}$ pixels. Basically, k_w and k_h characterize the kernel width and height correspondingly. Eq. (3) displays the convolution layer equation:

$$O_{x,y,q} = B_q + \sum_{i=1}^{c_{in}} \sum_{j=1}^{k_h} \sum_{k=1}^{k_w} Z_{x_{S+j}, y_{S+k}, i} \times W_{j,k,i,q} \tag{3}$$

where $O_{x,y,q}$, B_q, $Z_{x_{S+j}, y_{S+k}, i}$ and $W_{j,k,i,q}$ are a consequence of the convolution layer, specifically for pixel coordination (x, y) in q channel, bias, input from the preceding layer and a kernel value, correspondingly. The number of activation pixels that are moved after each convolution is adjusted as S [19].

C. Rectified Linear Unit (ReLU) Layer

In this layer, the activation function is ReLU. It offers a non-linear account by eliminating negative values and saving positive values from premium maps. Eq. (4) shows the calculation of ReLU.

$$R_{x,y,q} = f\left(O_{x,y,q}\right) = \max\left(0,\ O_{x,y,q}\right) \tag{4}$$

where the output of the layer is comprised of $R_{x,y,q}$ and max refers to the maximum operation [20].

D. Pooling Layer

This layer played an essential role in reducing the size of the input channels. ReLU outputs (maximum or average values) are extracted by the assembly layer. Thus, it reduces the size of particularities by assembling maximum values, according to the following Eq. (5):

$$P_{a^l, b^l, c} = \max_{0 \le a \le h_p, 0 \le b \le w_p} R_{a^l \times h_p + a, b^l \times w_p + b, c} \tag{5}$$

where a and b are iterators over the pooling window dimensions, and the layer output is $P_{a^l, b^l, c}$, $0 \le a^l < h_p^l$, $0 \le b_l < w_p^l$, $0 < c < c^l = c^{l-1}$; h_p^l is the height of a pooled channel; w_p^l is the width of a pooled channel; l and $l-1$ are correspondingly referring to the current and previous layers. w_p and h_p represent the successive width and height of the sub-region to be compiled from ReLU results [21].

E. Cross-Channel Normalization Layer

It offers the normalization of the local response through the channel, which is called brightness normalization. At every entrance of the assembly layer, the natural activation function is:

$$lrn^i_{a^l, b^l, c} = \frac{P^i_{a^l, b^l, c}}{\left(k + \alpha \sum_{j=\max(0, i-\frac{n}{2})}^{\min(N-1, i+\frac{n}{2})} \left(P^j_{a^l, b^l, c}\right)^2\right)^\beta} \tag{6}$$

where N is the total number of kernel maps in the layer, i is the applied kernel, and n is the number of neighboring kernel mappings for a given spatial point. k, α, β are constants, defined as follows:

k: A bias parameter to avoid division by zero.

α: A scaling parameter for the normalization.

β: The exponent for the normalization factor.

j: The iterator for summation within the normalization window [18].

F. Fully Connected Layer

It is devoted to mapping the number to the previous layer. The assembly layer and the necessary number of categories or outputs can be efficiently mapped by a completely connected layer. Eq. (7) fully reflects how the corresponding layer operates as follows:

$$F_r = \sum_{d=1}^{mc_1^{l-1}} \sum_{g=1}^{mc_2^{l-1}} \sum_{h=1}^{mc_3^{l-1}} W^l_{d,g,h,r} \left(lrn_c\right)_{d,g} \quad \forall \le mc^l \tag{7}$$

where: F_r refers to the fully connected layer outcome. mc_1^{l-1} and mc_2^{l-1} and mc_3^{l-1} respectively are dimensions of the input feature map from the layer $l-1$. A connected weight value between the preceding layer and the fully connected layer is $W^l_{d,g,h,r}$. The normalized output from the previous layer at position (d, g, h) is lrn for channel c, and the number of required neurons in the current layer (it can be equal to the number of required classes or outputs) is mc^l [22].

G. SoftMax Layer

It is used to estimate the rating possibilities for every input image. Eq. (8) refers to its activation function [22]:

$$S_r = \frac{e^{F_r}}{\sum_{s=1}^{mc^{l-1}} e^{F_s}}, \quad r = 1, 2, ..., mc^l \tag{8}$$

where:

S_r: The softmax output for the r-th class.

F_r: The fully connected layer output for the r-th neuron.

mc^{l-1} : the quantity of neurons in the layer that was previously totally linked.

e: The exponential function.

H. Classification Layer

The final determination of recognition or classification is made using it. The foundation of this layer is winner-take-all. Its function is represented by the Eq. (9):

$$CL_r = \begin{cases} 1 \ if \ S_r = Max \\ 0 \ otherwise \end{cases}, \ r = 1,2,...,mc^l \quad (9)$$

where: CL_r refers to the final decision of the classification layer, and the maximum value obtained from the softmax layer is denoted as max [23].

III. Related Works

The classification of WBCs types by the deep learning CNN technique has been the subject of many studies. Jiang *et al*. [24] presented the WBCNet system and the CNN architecture to classify the WBCs by their images from the optical microscope, which showed 33 layers of WBCNet and was compared with CNN to achieve the accuracy on the coaching group of 77.65% for best 1, 98.65% for best 5 and 83% for best 1 on exam group. Yildirim *et al*. [25] offered the classified images of WBCs types by connecting CNN with four networks: AlexNet, ResNet50, DenseNet201, and Google Net. The result of the study obtained a filtered image, which was better than the original image and can diagnose the hematology much easier.

Sharma *et al*. [26] provided the CNN regulation to classify the leukocytes through extracted manual and automated data sets from optical microscope instruments to produce an accuracy of 96% for a dual category and an accuracy of 87% for multiple categories. Shahin *et al*. [27] served as a CNN framework to define the white blood cells by the data extracted from the networks that primary training and uniformity order. In addition, two ways were used—transfer learning and fine-tuning—to get the result's accuracy of 96.1%. Kutlu *et al*. [28] submitted a detector that was for the classification of WBCs in the same image that was trained by CNN based on RCNN and compared with the AlexNet, VGG16, Google Net, and ResNet 50 architectures for full and transfer learning to produce the accuracy rates of 95.04% for neutrophil, 96.16% for eosinophil, 98.48% for basophil, 98.40% for monocyte and 99.52% for lymphocyte.

Al-Hatab *et al*. [29] extended the deep learning algorithm to compare the 3 axes of the Classification Model (CM) of functional magnetic resonance images: XCM, YCM, and ZCM, then compare them to categorize the assignments such as motion, visibility, and activity of the brain to procure the accuracy rate 91.67% for XCM, 89.88% for YCM and 91.67% for ZCM. Ali *et al*. [30] advanced the DL by using huge ear print data images to obtain an accuracy rate of 97.33% for left ear prints and 97.87% for right ear prints. Ekiz *et al*. [31] tendered the classification between four types of WBCs with CNN technique and Convolutional features Support Vector Machines (Con-SVM). The CNN technique resulted in an accuracy of 83.91% and the accuracy of Con-SVM scored 85.96%. Yıldırım and Çınar [32] chipped the CNN algorithm to classify the images of human movements by giving information about 40 various movements. The CNNs related to three networks: InceptionV3, Google Net, and AlexNet algorithms to reach an accuracy of 76.15 in InceptionV3. Eroğlu *et al*. [33] developed a hybrid CNN architecture to detect the mass lesion of the breast as benign or cancer by connecting the CNN with the AlexNet, MobileNetV2, and ResNet 50 systems to get 95.6% accuracy. Muhamad *et al*. [34] used the CNN system and SVM to classify the trained data images for two parts of WBCs as granular and non-granular WBCs to generate an accuracy rate of 98.4% for CNN and 90.6% for the SVM model. Shahzad *et al*. [35] exposed a CNN that used the characteristics of WBCs trained images with resNet50 and efficient NetBO models and SVM with Quadratic Discriminant Analysis (QDA). These algorithms were used to classify the eosinophil with an accuracy rate of 97.92%, the neutrophil with an accuracy rate of 96.8%, the lymphocytes with an accuracy rate of 99.84%, and the monocytes with an accuracy rate of 99.80%.

The purpose of this work is to propose the NDLM. The WBC types of neutrophils, basophils, eosinophils, lymphocytes, and monocytes are classified using train image data. It has been demonstrated that the NDLM performs better. Furthermore, the accuracy outcomes of the proposed model are contrasted with those of prior investigations concerning the classification of WBC kinds.

IV. Implementation

Matlab was chosen for NDLM implementation because of its extensive use in AI and image processing applications. Matlab's multi-paradigmatic nature, efficiency, and extensive library make working with neural networks a breeze. The network is built from the ground up, beginning with the convolution and normalization layers and progressing to the classification layer, albeit it occasionally makes use of these libraries' features. The area of Artificial Neural Networks (ANNs) known as machine learning uses a collection of samples to train the neural system's structure. Deep learning, which is a sub-branch of machine learning, is used to learn and understand information extracted from computer data as a sequence of pyramidal [36]. Deep learning is used in biomedical image and signal processing. In this study, NDLM is suggested to classify the WBC images according to their types. It can be considered as a developed CNN. This suggested model (NDLM) consists of many layers explained in the architecture shown in Fig. 2.

Deep learning is one of the latest and wide-by-use areas of machine learning that lets computer devices manipulate, learn, and know of data whence a pyramid sequence. Machine learning has several branches/methodologies and deep learning is one of them, in which all algorithms are designed according to the texture and actions of the brain and called an intelligent neural network [37]. Images, videos, and biomedicine images/signals manipulation, and

classification, are examples of the domains in which deep learning is commonly used.

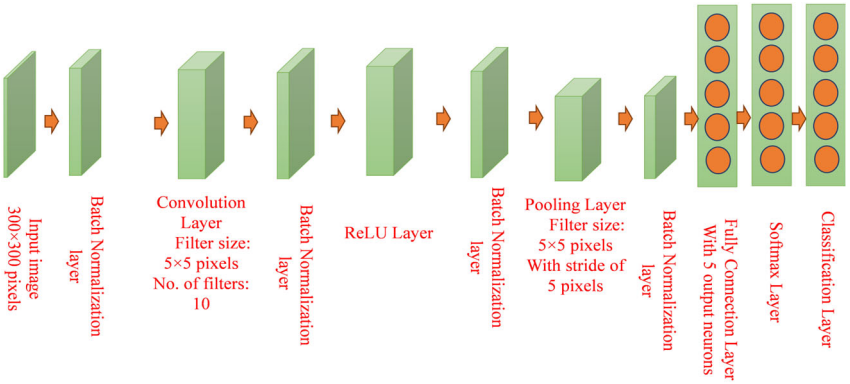

Fig. 2. Architecture of the suggested NDLM.

Significant trait that characterizes deep learning is that it can play with various layers, whilst in a classic ANN, every individual cell is linked to all other cells in the previous and subsequent layers. In each layer, several mathematical operations are implemented. Due to the increasing number of layers and data size, a high-quality of processing unit is required. Kermany *et al*. [38] show that GPU-powered and memory-intensive processors have a priority for DL. DL networks come in various forms, including CNNs, RNNs, long term memory networks, and deep auto-encoders.

V. Experimental Analysis

All experiments were conducted on a computer with the following specifications: a Dell laptop featuring an Intel (R) Core (TM) i5-8400H CPU operating at 2.50GHz and 16 GB of Random-Access Memory (RAM).

The NDLM network specs are as follows: the input picture dimensions are 300×300×3 pixels, the convolution layer has a 5×5-pixel filter with 10 filters, the maximum pooling size is 5×5 pixels, and the stride value is 5 pixels.

Adaptive Moment Estimation (Adam) optimizer, maximum epochs of 100, initial learning rate of 0.0010, decay rate of gradient moving average of 0.9, decay rate of squared gradient moving average of 0.999, and denominator offset of 10^{-8} are the parameters used in the DL network training process.

Fig. 3 illustrates two curves: One representing the correlation between successful accuracy and training iterations, and the other depicting the association between mini-batch loss and training iterations.

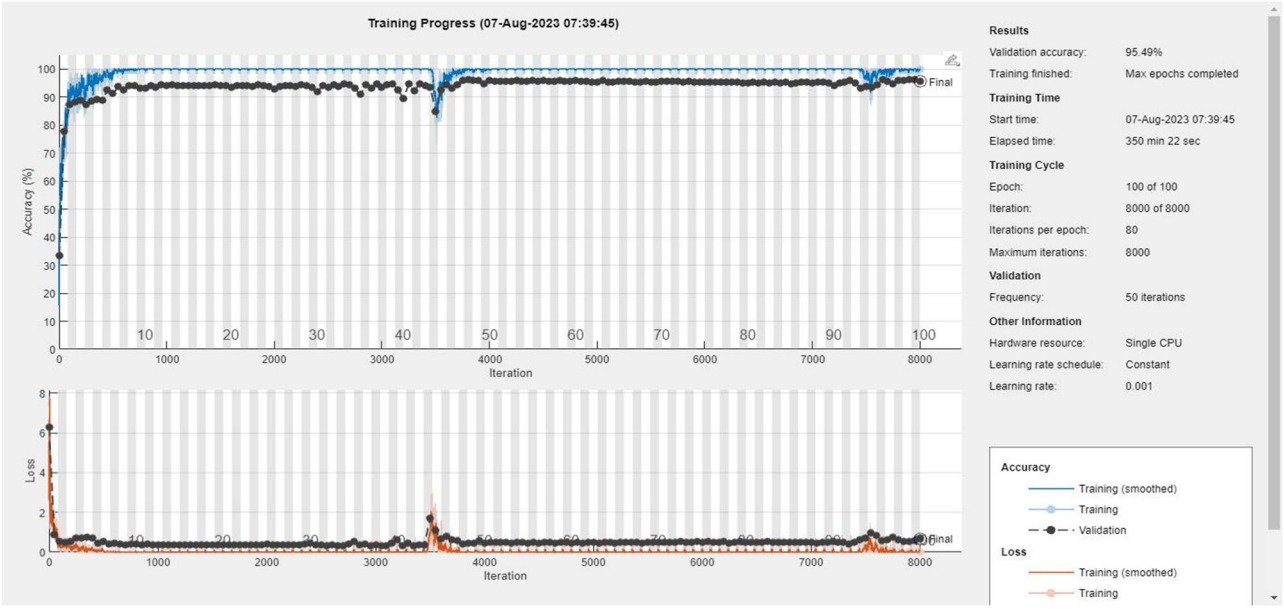

Fig. 3. Learning curves for the NDLM with 100 iterations.

Further results of training can be seen in Fig. 3, in which the total training time for DL is 5 h, 50 min and 22 s. A successful overall accuracy have been achieved, with a low error of 3.81 obtained, as shown in Table I.

TABLE I. NDLM Testing Results

Method	Overall accuracy (%)	Errors
NDLM	96.19%	3.81

This study demonstrated how to keep an NDLM network's parameter count as low as required without sacrificing accuracy. In the filtering layer, the parameters were 5×5 pixels and there were 10 filters; in the assembly layer, the parameters were 5×5 pixels and there were 5 filters. This model analyzed or inspected the parameters extensively.

A. The Performance Measures of Classifying White Blood Cell Subtypes

The Classification performance for different subtypes of White Blood Cells (WBC) shows high accuracy in all measurements, as shown in Table II. Eosinophils obtain near-perfect results, with a precision of 0.99, sensitivity of 0.98, specificity of 1.00, and an F1-Score of 0.99, indicating exceptional reliability in identifying this subtype. Neutrophils also show impressive performance, with an accuracy of 0.98 and an F1-Score of 0.97, reflecting high consistency. Lymphocytes and basophils give balanced performance, each maintaining accuracy and sensitivity above 0.90, with a specificity of 0.99. Monocytes, although having the lowest resolution at 0.89, are compensated for by a high sensitivity of 0.95 and a solid F1-Score of 0.92.

In general, the model shows robust classification capabilities, particularly for eosinophils and neutrophils, with minimal misclassification across all subtypes.

TABLE II. THE PERFORMANCE MEASURES OF CLASSIFYING WBC DATASET IN NDLM MODEL

WBC Subtype	Precision	Sensitivity	Specificity	F1- Score
Basophil	0.91	0.93	0.99	0.92
Eosinophil	0.99	0.98	1	0.99
Lymphocyte	0.94	0.93	0.99	0.94
Monocyte	0.89	0.95	0.98	0.92
Neutrophil	0.98	0.96	0.99	0.97

B. The Comparative Analysis between Normalized Deep Learning Model (NDLM) and Other Networks

In order to improve this paper and illustrate the potential benefits and limitations of using NDLM, our White Blood Cell (WBC) data was fed into many DL networks with various models and parameters, and in-depth comparisons were conducted between them and our NDLM network. Table III provided these comparisons based on accuracy. You can see that the model we created had the best categorization resolution.

TABLE III. COMPARISONS WITH METHODS THAT CONSIDER WBC REGIONS

Reference	Method	Accuracy (%)	Errors
[39]	DFCN	94.56	5.44
[30]	DL	94.76	5.24
[40, 41]	DFTL	94.7	5.3
[42]	CDFL	90.64	9.36
[43]	NDEL	95.69	4.31
[44]	ResNet	95.22	4.78

The first model to compare with was Deep Fingerprint Classification Network (DFCN). This model has widely evaluated or inspected parameters. The parameters in the convolutional layer were a filter size of 5×5 pixel and the number of filters was 8, while in the pooling layer, the filter size was 5×5 pixel and the stride was 5 [39].

While in the second architecture that we compared our architecture with, Deep Learning (DL), the highest accuracy in this case was 94.76%. The layers were composed of a single convolution with a filter size of 15×15 pixels and the number of filters: 10, single ReLU, single pooling where pooling size: 5×5 pixel and the stride: 5, fully connected, softmax, and classification layers [16].

In the third comparison, the comparison was with research that considered Deep Finger Texture Learning (DFTL) as one of such techniques where the CNN. Unlike the CNN in other research, there was no need to repeat the layers. For example, only one ReLU layer and one convolution layer should be present. The Finger Texture (FT) patterns' straightforward explanations of both horizontal and vertical patterns are the reason behind this. As a result, it greatly simplified the algorithm and boosted its performance, the accuracy was 94.7% [40].

This model layers are also composed of a single convolution with a filter size of 15×15 pixels and the number of filters: 10, single ReLU, single pooling, fully connected were pooling size: 5×5 pixel and the stride: 5, SoftMax, and classification layer [40].

On the other hand, the study was compared against the Couple of Deep Finger-photos Learning (CDFL) technique that has been suggested, which involved a couple of DL networks, each convolution layer with a filter size of 5×5 pixels and the number of filters: 2, single ReLU, single pooling, fully connected were pooling size: 7×7 pixel and the stride: 3, softmax, and classification layers, the accuracy was 90.64% [42].

Batch normalization, convolution, ReLU, pooling, cross-channel normalization, fully linked, softmax, and classification layers are the successive components of the NDEL layers in the fifth comparison. The normalization layer had a window channel size of 7, while the convolutional layer had a filter size of 15×15 pixels, 10 filters, a single ReLU, single pooling, completely linked, pooling size of 5×5 pixels, and stride size of 5 [43].

We compared with a DDFL network. It also consisted of two Deep Learning (DL) networks, while also each convolution layer with filter size of 15×15 pixels, the number of filters: 10, and fully connected were pooling size: 5×5 pixel and the stride: 5 [41].

TABLE IV. THE PERFORMANCE MEASURES OF CLASSIFYING WBC DATASET IN RESNET-MODEL

WBC Subtype	Precision	Sensitivity	Specificity	F1-Score
Basophil	0.97	0.94	1	0.96
Eosinophil	0.94	0.97	0.97	0.95
Lymphocyte	0.94	0.96	0.99	0.95
Monocyte	0.97	0.88	1	0.92
Neutrophil	0.96	0.96	0.98	0.96

Finally, we performed a comparative experiment utilizing a Matlab-based implementation of a ResNet-like model as published by Chen *et al*. [44] to assess the performance of our suggested model versus popular designs. The results revealed that our model obtained

superior classification accuracy (95.22%) across all five white blood cell types. Table IV provides a summary of the specific metrics for each class, such as precision, recall, and F1-Score.

Although both models show excellent accuracy for every WBC subtype, they differ in a few key areas.

- For Eosinophils and neutrophils, NDLM exhibits higher sensitivity and F1-Scores, suggesting a better trade-off between recall and precision.
- ResNet typically exhibits more specificity and precision, particularly for monocytes and basophils.

C. White Blood Cell (WBC) Dataset

The blood picture has white blood cells, red blood cells, and platelets. The data set of blood images have been obtained in the color space RGB that is acquired from the analyzer CellaVision, DM96. The data of blood pictures contain 17,092 images with size 360×363 pixels and formatted in jpg. Otherwise, the data of WBCs types as: neutrophils, basophils, eosinophils, lymphocytes, and monocytes that acquired from the blood picture to classify the WBCs types [45].

In preprocessing, before inserting images into the model, all images were resized to a uniform dimension of 300×300 pixels to ensure consistency of the input data and compatibility with the model structure.

D. Data Separation and Validation Strategy

The dataset used in our experiments was stratified, with 50% going to training, 25% to validation, and 25% to testing. In all five WBC categories, this ensured fair representation. The test set was chosen for the final analysis, while the validation set was used to evaluate model performance and modify hyperparameters.

Future studies will look at how cross-validation impacts the model's generalizability. However, it was not done due to computational constraints.

VI. Conclusion

WBC images are classified for neutrophils, basophils, eosinophils, lymphocytes and monocytes types. The data are classified by a suggested NDLM, which can be considered as a developed CNN and it is a type of deep learning. It contains the several layers of batch normalization, cross channel normalization, convolution, batch normalization, ReLU, batch normalization, pooling, batch normalization, fully connected, SoftMax, and classification layers. Such structure is intensively discovered, assessed and confirmed. The main results in this paper are an accuracy equal to 96.19% and a low error equal to 3.81%. Comparisons were also considered in this study, where the suggested model attained superior performance.

The real practical significance of the model is shown in the automated classification of white blood cells in digital blood slide analysis tools, which integrate the NDLM model into the hematology process. Medical intervention will accelerate by reducing the requirement for physical inspection and connecting it to computerized patient information to spot anomalous patterns and give early warning signs for diseases like leukemia or infection.

Regarding accuracy and reliability, when compared to hematologists, the model has occasionally achieved accuracy that surpasses or is comparable to the performance of doctors. This is because the model is not impacted by human bias or fatigue, which gives it a high capacity for repetition and consistency in results.

Additionally, unlike doctors, who have a rather set knowledge base, the model will have modified with fresh data on a regular basis, enabling it to stay up to date with the most recent diagnostic criteria.

Conflict of Interest

The authors declare no conflict of interest.

Author Contributions

The experiments were devised, and the code was implemented by Neam S. M. Sh. and Raid Rafi. The entire production was managed by Ali R. H. Aljader and Mazin N. Farhan, who also provided ideas for the article. The paper was written by Ali R. H. Aljader, Neam S. M. Sh., Mazin N. Farhan, and Raid R. O. Al-Nima, who also gave their final approval. The last version had been approved by all authors.

References

[1] R. Asghar, S. Kumar, P. Hynds, and A. Shaukat, "Classification of white blood cells using machine and deep learning models: A systematic review," arXiv Print, arXiv:2308.06296, 2023. doi: 10.48550/arXiv.2308.06296

[2] O. Sarrafzadeh, H. Rabbani, A. Talebi, and H. U. Banaem, "Selection of the best features for leukocytes classification in blood smear microscopic images," in *Proc. Medical Imaging 2014: Digital Pathology*, 2014, vol. 9041, pp. 159–166.

[3] T. Lange, F. Luebber, H. Grasshoff *et al*., "The contribution of sleep to the neuroendocrine regulation of rhythms in human leukocyte traffic," *Seminars in Immunopathology*, vol. 44, no. 2, pp. 239–254, 2022.

[4] Y. Liu, Y. Liu, M. Chen *et al*., "Automatic recognition of blood cell images with dense distributions based on a faster region-based convolutional neural network," *Applied Sciences*, vol. 13, no. 22, 12412, 2023.

[5] S. S. Vellela *et al*., "A blood cell classification using a deep learning algorithm CNN," *International Journal of Emerging Technologies and Innovative Research*, vol. 5, no. 2, pp. 258–263, 2018.

[6] A. A. Hasanaath, A. S. Mohammed, G. Latif *et al.*, "Acute lymphoblastic leukemia detection using ensemble features from multiple deep CNN models," *Electronic Research Archive*, vol. 32, no. 4, 2024.

[7] Z. Jan, M. Shabir, H. Farman, A. Rahman, and M. M. Nasralla, "Deep learning based semantic segmentation of leukemia effected white blood cell," *PLoS One*, vol. 20, no. 5, e0320596, 2025.

[8] M. Shahzad, F. Ali, S. H. Shirazi *et al*., "Blood cell image segmentation and classification: A systematic review," *PeerJ Computer Science*, vol. 10, e1813, 2024.

[9] I. Mohammadzadeh, B. Niroomand, B. Hajikarimloo *et al.*, "Can we rely on machine learning algorithms as a trustworthy predictor for recurrence in high-grade glioma? A systematic review and meta-analysis," *Clinical Neurology and Neurosurgery*, vol. 249, 108762, 2025.

[10] M. A. Habibi, H. Amani, M. S. Mirjani and A. Molla, "Predicting the radiological outcome of cerebral aneurysm treatment with machine learning algorithms; a systematic review and diagnostic meta-analysis," *Interdisciplinary Neurosurgery*, vol. 36, 101929, 2024.

[11] B. Hajikarimloo, I. Mohammadzadeh, M. A. Habibi *et al*., "Deep learning-based models for ventricular segmentation in hydrocephalus: A systematic review and meta-analysis," *World Neurosurgery*, vol. 198, 124001, 2025.
[12] P. Urbaniak, S. Wronski, J. Tarasiuk *et al*., "A new method to estimate 3D cell parameters from 2D microscopy images," *Biochimica et Biophysica Acta (BBA)-Molecular Cell Research*, vol. 1869, no. 9, 119286, 2022.
[13] N. Zeng, H. He, V. V. Tuchin *et al*., "Tissue optical clearing for Mueller matrix microscopy," in *Proc. Handbook of Tissue Optical Clearing*, 2022, pp. 31–66.
[14] A. Shrestha and A. Mahmood. "Review of deep learning algorithms and architectures," *IEEE Access*, vol. 7, pp. 53040–53065, 2019.
[15] A. Acevedo, A. Merino, S. Alférez *et al*., "A dataset of microscopic peripheral blood cell images for development of automatic recognition systems," *Data in Brief*, vol. 30, 105474, 2020.
[16] H. H. Mohammed, S. A. Baker, and O. I. Alsaif. "An improved underwater image enhancement approach for border security," *Journal of Image and Graphics*, vol. 12, no. 2, pp. 199–204, 2024.
[17] S. Albawi, T. A. Mohammed, and S. A. Zawi. "Understanding of a convolutional neural network," in *Proc. 2017 International Conference on Engineering and Technology (ICET)*, 2017.
[18] T. F. Gonzalez, *Handbook of Approximation Algorithms and Metaheuristics*, Chapman and Hall/CRC, 2007.
[19] A. Ardakani, C. Condo, M. Ahmadi, and W. J. Gross, "An architecture to accelerate convolution in deep neural networks," *IEEE Transactions on Circuits and Systems I: Regular Papers*, vol. 65, no. 4, pp. 1349–1362, 2017.
[20] Y. Zhang, J. Gao, and H. Zhou. "Breeds classification with deep convolutional neural network," in *Proc. 12th International Conference on Machine Learning and Computing*, 2020, pp. 145–151.
[21] K. O'Shea and R. Nash, "An introduction to convolutional neural networks," arXiv Print, arXiv:1511.08458, 2015. doi: 10.48550/arXiv.1511.08458
[22] N. Otsu, "A threshold selection method from gray-level histograms," *Automatica*, vol. 11, no. 285–296, pp. 23–27, 1975.
[23] R. R. O. Al-Nima, "Signal processing and machine learning techniques for human verification based on finger textures," Ph.D. dissertation, Newcastle University, UK, 2017.
[24] M. Jiang, L. Cheng, F. Qin, L. Du, and M. Zhang, "White blood cells classification with deep convolutional neural networks," *International Journal of Pattern Recognition and Artificial Intelligence*, vol. 32, no. 9, 1857006, 2018.
[25] M. Yildirim and A. Çinar, "Classification of white blood cells by deep learning methods for diagnosing disease," *Rev. d'Intelligence Artif.*, vol. 33, no. 5, pp. 335–340, 2019.
[26] M. Sharma, A. Bhave, and R. R. Janghel, "White blood cell classification using convolutional neural network," in *Proc. Soft Computing and Signal Processing*, 2019, pp. 135–143.
[27] A. I. Shahin, Y. Guo, K. M. Amin, and A. A. Sharawi, "White blood cells identification system based on convolutional deep neural learning networks," *Computer Methods and Programs in Biomedicine*, vol. 168, pp. 69–80, 2019.
[28] H. Kutlu, E. Avci, and F. Özyurt, "White blood cells detection and classification based on regional convolutional neural networks," *Medical Hypotheses,* vol. 135, 109472, 2020.
[29] M. M. AL-Hatab, R. R. O. Al-Nima, I. Marcantoni *et al*., "Comparison study between three axis views of vision, motor and pre-frontal brain activities," *Journal of Critical Reviews*, vol. 7, no. 5, pp. 2598–2607, 2020.
[30] S. O. Ali, R. R. Al-Nima, and E. A. Mohammed, "Individual recognition with deep earprint learning," in *Proc. 2021 International Conference on Communication & Information Technology (ICICT)*, 2021, pp. 304–309.
[31] A. Ekiz, K. Kaplan, and H. M. Ertunç, "Classification of white blood cells using CNN and Con-SVM," in *Proc. 2021 29th Signal Processing and Communications Applications Conference (SIU)*, 2021, pp. 1–4.
[32] M. Yıldırım and A. Çınar, "Classification of 40 different human movements with CNN architectures and comparison of their performance," *Turkish Journal of Science and Technology*, vol. 16, no. 1, pp. 103–112, 2021.
[33] Y. Eroğlu, M. Yildirim, and A. Çinar, "Convolutional neural networks based classification of breast ultrasonography images by hybrid method with respect to benign, malignant, and normal using mRMR," *Computers in Biology and Medicine*, vol. 133, 104407, 2021.
[34] H. A. Muhamad, S. W. Kareem, and A. S. Mohammed, "A comparative evaluation of deep learning methods in automated classification of white blood cell images," in *Proc. 2022 8th International Engineering Conference on Sustainable Technology and Development (IEC)*, 2022, pp. 205–211.
[35] A. Shahzad, M. Raza, J. H. Shah *et al.*, "Categorizing white blood cells by utilizing deep features of proposed 4B-AdditionNet-based CNN network with ant colony optimization," *Complex & Intelligent Systems*, vol. 8, no. 4, pp. 3143–3159, 2022.
[36] M. Chen, U. Challita, W. Saad *et al.*, "Artificial neural networks-based machine learning for wireless networks: A tutorial," *IEEE Communications Surveys & Tutorials*, vol. 21, no. 4, pp. 3039–3071, 2019.
[37] T. Y. Abdulqader, S. A. Abdulqader, and S. A. Baker, "Enhancing image recognition with quaternion neural networks: A novel approach to color layer integration," *Journal of Image and Graphics*, vol. 13, no. 2, pp. 190–197, 2025.
[38] D. S. Kermany, M. Goldbaum, W. Cai *et al.*, "Identifying medical diagnoses and treatable diseases by image-based deep learning," *Cell*, vol. 172, no. 5, pp. 1122–1131, 2018.
[39] A. M. Ibrahim, A. K. Eesee, and R. R. O. Al-Nima, "Deep fingerprint classification network," *Telecommunication Computing Electronics and Control*, vol. 19, no. 3, pp. 893–901, 2021.
[40] R. R. Omar, T. Han, S. A. Al-Sumaidaee, and T. Chen, "Deep finger texture learning for verifying people," *IET Biometrics*, vol. 8, no. 1, pp. 40–48, 2019.
[41] R. R. O. Al-Nima, S. Q. Hasan, and S. Esmail, "Exploiting the deep learning with fingerphotos to recognize people," *International Journal of Advance Science and Technology*, vol. 29, no. 7, pp. 13035–13046, 2020.
[42] R. R. O. Al-Nima, S. Q. Hasan, and S. E. Mahmood, "Utilizing fingerphotos with deep learning techniques to recognize individuals," *NTU Journal of Engineering and Technology*, vol. 2, no. 1, 2023.
[43] S. O. Ali, R. R. O. Al-Nima, and E. A. Mohammed, "Communication establishment based on authenticating earprints," *International Journal of Future Generation Communication and Networking*, vol. 14, no. 1, pp. 3242–3264, 2021.
[44] H. Chen, J. Liu, C. Hua *et al*., "Accurate classification of white blood cells by coupling pre-trained ResNet and DenseNet with SCAM mechanism," *BMC Bioinformatics*, vol. 23, no. 1, p. 282, 2022.
[45] A. Acevedo, A. Merino, S. Alférez *et al*., "A dataset of microscopic peripheral blood cell images for development of automatic recognition systems," *Data in Brief*, vol. 30, 105474, 2020.